Obrabotka metallov (tekhnologiya, oborudovanie, instrumenty) = Metal Working and Material Science. 2018 vol. 20 no. 3 pp. 109–122
ISSN: 1994-6309 (print) / 2541-819X (online)
DOI: 10.17212/1994-6309-2018-20.3-109-122

Obrabotka metallov -
Metal Working and Material Science

Journal homepage: http://journals.nstu.ru/obrabotka_metallov

Optimization of Molybdenum Powder Milling Parameters

Dyčková Lucie [1, a], ***Komarov Pavel*** [1, 3, b, *], ***Remešová Michaela*** [1, c], ***Dyčka Martin*** [1, d], ***Dvořák Karel*** [2, e], ***Menelaou Melita*** [1, f], ***Čelko Ladislav*** [1, g]

[1] Brno University of Technology, Central European Institute of Technology, 123 Purkynova st., Brno, 61200, Czech Republic
[2] Brno University of Technology, Faculty of Civil Engineering, 512/95 Veveří st., Brno, 60200, Czech Republic
[3] Novosibirsk State Technical University, 20 Prospekt K. Marksa, Novosibirsk, 630073, Russian Federation

[a] http://orcid.org/0000-0003-1814-059X, lucie.palenikova@ceitec.vutbr.cz, [b] http://orcid.org/0000-0002-6854-4536, pavel.komarov@ceitec.vutbr.cz,
[c] http://orcid.org/0000-0003-1678-5618, michaela.remesova@ceitec.vutbr.cz, [d] http://orcid.org/0000-0001-6419-253X, martin.dycka@ceitec.vutbr.cz,
[e] http://orcid.org/0000-0003-2111-3357, dvorak.k@fce.vutbr.cz, [f] http://orcid.org/0000-0001-7845-8802, melita.menelaou@ceitec.vutbr.cz,
[g] http://orcid.org/0000-0003-0264-3483, ladislav.celko@ceitec.vutbr.cz

ARTICLE INFO

Article history:
Received: 10 June 2018
Revised: 28 June 2018
Accepted: 15 August 2018
Available online: 15 September 2018

Keywords:
Molybdenum powder
High energy milling
Ball to powder weight ratio (BPR)
Rotational speed
Milling time
Particle size

Funding:
This research has been financially supported by the Ministry of Education, Youth and Sports of the Czech Republic under the project CEITEC2020 (LQ1601).

Acknowledgements:
We also acknowledge CEITEC Nano Research Infrastructure (ID LM2015041) for providing us with access to its SEM devices.

ABSTRACT

Introduction. The refractory materials are of interest for high temperature applications in aerospace, nuclear and military industries, since they possess high melting temperature (> 2000 ˚C). Molybdenum (Mo) is among these materials of high interest due to its excellent properties such as good thermal conductivity, high strength and toughness. The production of molybdenum is difficult due to its high melting point and the temperature of the ductile-brittle transition, therefore, in the production of this metal, powder metallurgy methods are mainly used. To implement these methods, it is necessary to have high-quality molybdenum powders, in particular, a high degree of purity and homogeneity of particle size distribution. One of the powder processing methods that is used to produce nano- and microsize powders, is the high energy kinetic milling. This cost-effective method is based on the friction and the high-energy collisions between the balls and the powder particles. And therefore, **the purpose of the current work** is to optimize the parameters of high energy kinetic milling for molybdenum powder. Optimization of processing parameters has a significant influence on the acceleration of the process of product formation, on subsequent sintering and achievement of the best mechanical properties of the final product. Optimization of milling parameters of Mo powder was achieved under different milling parameters including among others the rotation speed, the ball to powder weight ratio (BPR) and the milling time. Initially, the rotational speed was determined; it varied from 600 to 1200 rpm (where rpm are revolutions per minute). After this determination, milling parameters such as the milling time and the BPR were varied. The milling time ranged from 2 to 60 min and the BPR varied from 100:3 to 200:3. After that, influence of variable parameters on morphology and powder particles size distribution was investigated. The initial powder used in these experiments was Mo powder (particle size ~100 μm). **The methods of investigation**. Scanning electron microscopy and laser diffraction methods were used to estimate the particle size distribution. **Results and Discussion**. Particle size was decreased from 100 to 4 μm with increasing grinding time from 2 to 60 min. However, in each batch, a number of cold-welded particles measuring 200-400 μm was detected. These cold-welded particles were about 200-400 μm in size. As the result, the optimal milling parameters were: rotation speed of 900 rpm, BPR (200:3) and milling time of 60 minutes.

For citation: Dyčková L., Komarov P., Remešová M., Dyčka M., Dvořák K., Menelaou M., Čelko L. Optimization of molybdenum powder milling parameters. *Obrabotka metallov (tekhnologiya, oborudovanie, instrumenty) = Metal Working and Material Science*, 2018, vol. 20, no. 3, pp. 109–122. doi: 10.17212/1994-6309-2018-20.3-109-122. (In Russian).

*** Corresponding author**
Komarov Pavel, Ph.D. (Engineering) student
Brno University of Technology,
Purkynova 123,
61200, Brno, Czech Republic
Tel.: 420 777-840-687, **e-mail:** pavel.komarov@ceitec.vutbr.cz

Introduction

Molybdenum (Mo) is an important refractory metal due to one of the highest melting points among all the metals (T_m=2612 °C), [1]. It has good thermal conductivity (138 W·m-1·C-1) and low specific heat (25.1-28.4 J·K-1·mol-1 at 400-100 K), [2]. Also, it possesses high strength and toughness; for instance, the high-temperature strength of the unalloyed molybdenum is of about 50 MPa at 1000 °C, while the high-temperature strength of the alloyed molybdenum is approximately 900 MPa at the same temperature [3]. Therefore, molybdenum is used for high temperature applications in power energetics and thermal spray coatings [1, 4]. The main technique for its fabrication process is powder metallurgy; it can overcome disadvantages of other manufacturing processes and can also produce a fine-grained microstructure [5]. Two main disadvantages of molybdenum fabrication processes are the ultra-high melting temperature and the ductile-to-brittle transition temperature (DBTT) which can be at or even below room temperature [5, 6]. Moreover, spherical shape molybdenum powder is widely used in thermal spraying where the spherical shape ensures good flowability and high apparent density [7]. The coatings formed using spherical molybdenum powders are denser, more uniform and have better wear resistance. Furthermore, another possible way of the molybdenum bulk components production is sintering. The easier sintering and better mechanical properties of molybdenum are generally achieved with the smaller powder particle size [8]. It's a common knowledge that grain boundaries of molybdenum alloys affect mechanical properties, such as high strength and ductility, whereas the better mechanical properties are attained by smaller grain size and small impurity concentration (i.e. O, N) at grain boundaries [9]. For production of molybdenum, it is important to use high-quality molybdenum powders in purity, particle agglomeration and homogenous particle size distribution. Products made of these powders exhibit higher yield strength, higher tensile strength and lower elongation at room temperature [10]. On the other hand, molybdenum powder produced by conventional technique, such as hydrometallurgy or pyrometallurgy, has many defects, for example high scatter in non-uniformity of powder particle size [7-14].

High energy kinetic milling is a cost-effective method for the production of nanocrystalline or amorphous materials, consisting of equilibrium and/or non-equilibrium phases. It is a solid-state powder processing technique in which the size of the coarse powder particles is reduced to micrometer size [15-19]. High energy kinetic milling was originally developed for the production of oxide-dispersion strengthened (ODS) alloys based on iron or nickel [20]. During milling process the powder particles are subjected to high-energy collisions with the balls, so the particles are repeatedly deformed, welded and fractured [21]. The powder particle size is refined since the required particle size is reached. Until that time, the balance between the welding and fracturing of powder particles is not achieved. The milling process is dramatically influenced by type, shape, weight and size of the balls. Other significant parameters are the milling time, milling speed, milling atmosphere, milling container, milling medium, temperature and the charge ratio [22]. The ball to powder weight ratio is a crucial variable which influences the acceleration of the formation of products and also the change in the resultant phases for the powder mixture. For each successful milling process, the determination of the ball to powder weight ratio is needed. A significant part in the contamination issue of the final product is played by the milling balls and the milling container [22, 23]. It is also crucial to have optimal milling parameters because along with subsequent sintering, the increased mechanical properties can be obtained [23].

Thus, the main objective of this study was to investigate and determine the optimized high energy milling parameters of the Mo powder. To the beat of our knowledge such studies have not been reported while several publications exist that deal with understanding the milling parameters, the microstructure and the morphology of Mo-alloys (e.g. Co-Cr-Mo alloy). The effect of milling variables on the particle size was evaluated for different parameters taking into account: (i) rotational speeds, (ii) BPRs, and (iii) milling time.

Methodology of the study

Molybdenum powder (30.63.2, GTV GmbH, Germany) was supplied in agglomerated and sintered state. The chemical composition of this powder was 99.0 wt.% molybdenum, 0.1 wt.% oxygen and 0.9 wt.% impurities. The particles had the form of irregular spheres and were of about 100 μm in size. Representative scanning electron microscopy images (SEM-BSE) are shown in Fig. 1. In particular, the typical initial powder is shown in Figure 1a and the detail of a single powder particle is in Figure 1b.

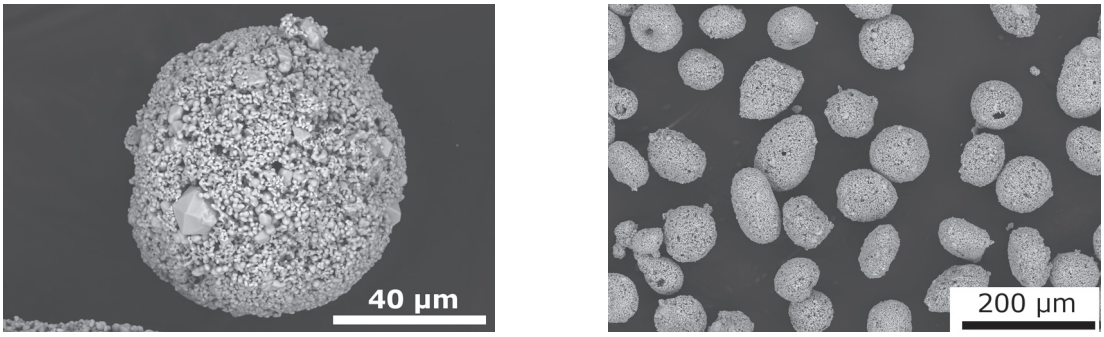

a *b*

Fig. 1. Morphology of Mo powder (*a*) and the detailed image of a single Mo particle (*b*)

All experiments were carried out using the high energy kinetic mill Simoloyer CM-01 (Zoz GmbH, Germany), where steel balls of 5 mm in diameter were used as a grinding media. The weight of the initial powders was kept constant (30 g) for all the experiments. Within each load, polyethylene glycol (PEG) (15-20 drops) (0.5 mL) was added into the mill container. PEG was used as one of the safe grinding assisting agents (liquid-assisted grinding) since it is an eco-friendly solvent which can help keep a cleaner reaction profile as well. The initial experiments for the determination of the rotational speed were carried out with the same BPR (100:3) and the same milling time (10 min). The rotational speeds were varied from 600 to 1200 rpm, see S1-S3 in Table 1.

Following that, the milling parameters such as the milling time and the BPR were also changed. The milling time ranged from 2 to 60 min. The balls weight was also design to differ, i.e. 1000 g and 2000 g; i.e. the BPR was 100:3 or 200:3. Detailed description of all samples for this experiment is summarized in Table.

Table 1

Detailed description of the milling parameters

Specimen	Rotational speed [rpm]	Time [min]	BPR [–]
S1	600	10	100:3
S2	900	10	100:3
S3	1200	10	100:3
1A	900	2	100:3
2A	900	5	100:3
3A	900	10	100:3
4A	900	30	100:3
5A	900	60	100:3
6B	900	2	200:3
7B	900	5	200:3
8B	900	10	200:3
9B	900	30	200:3
10B	900	60	200:3

The analysis and evaluation of milled powders were carried out via scanning electron microscopy (Verios; Thermo Fisher Scientific, Czech Republic) and laser diffraction study for the determination of powder particle size was implemented with Mastersizer 2000 (Malvern Instruments Ltd., England).

Results and discussions

The first milling parameter to be determined was the rotational speed which was set to: (i) 600 rpm, (ii) 900 rpm, and (iii) 1200 rpm, respectively. The milling time (10 min) and the BPR (100:3) were kept constant. For each milling batch, the typical powder morphologies are shown in Figure 2.

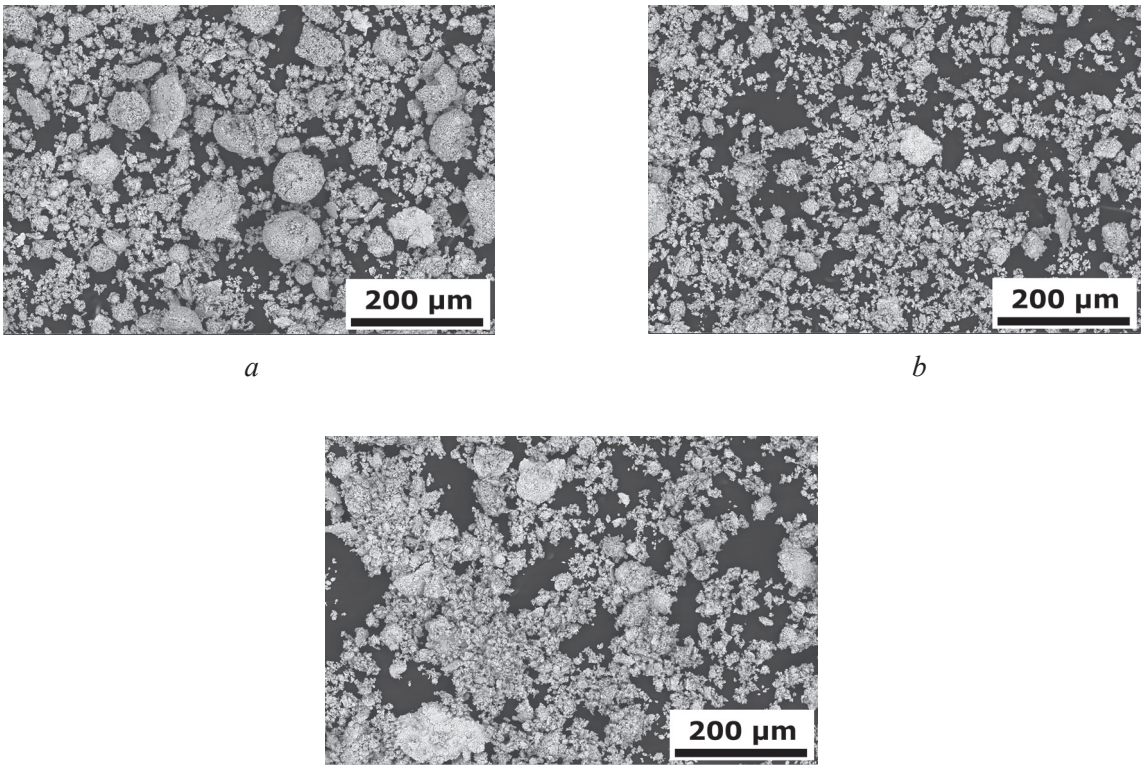

a *b* *c*

Fig. 2. High energy milled molybdenum powder with variation in rotational speed:
a – 600 rpm; *b* – 900 rpm; *c* – 1200 rpm, SEM-BSE

At the lowest rotational speed (600 rpm), the most agglomerated powder particles were partially broken through the repeated deformations and fractures. However, there was still a certain amount (~32 vol.%) of the agglomerated particles that remained the same in size as initial powder (Figures 3 and 4). For these milling parameters, there weren't observed any bigger cold-welded particles than initial ones.

At a higher rotational speed (900 rpm), most of initial particles were totally fractured. Some of them were plastically deformed and cold-welded. The efficiency of the milling process was higher than in the previous case, so there were very fine powder particles presented in this batch (see Figure 2b). The largest amount (up to 60 vol.%) of these particles was in the size range from 2 to 20 μm as shown in Fig. 3. The amount of the agglomerated particles with the same size as the initial was approximately up to 10 vol.% (see Figure 4). Cold-welded particles (13 vol.%) in the size range of 200-600 μm were also produced.

The highest milling speed (1200 rpm) exhibited also fine particles (see Figure 2c), but the amount (up to ~11 vol.%) of these particles in the size range of 12-20 μm was lower once compared with the findings at 900 rpm. The particles (35 vol.%) were more plastically deformed so they were flake-like in shape. Due to the flake-like morphology, it can be assumed, that the cold-welding process was minimized and the high

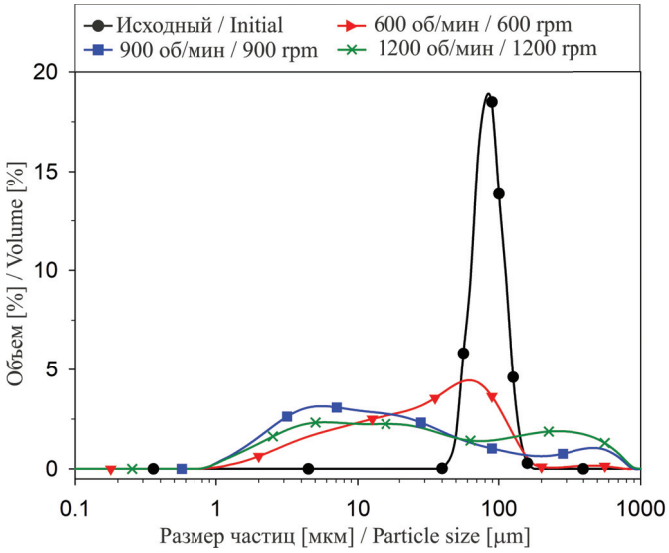

Fig. 3. The effect of the rotational speed on the particle size of initial molybdenum powder, BPR = 100:3

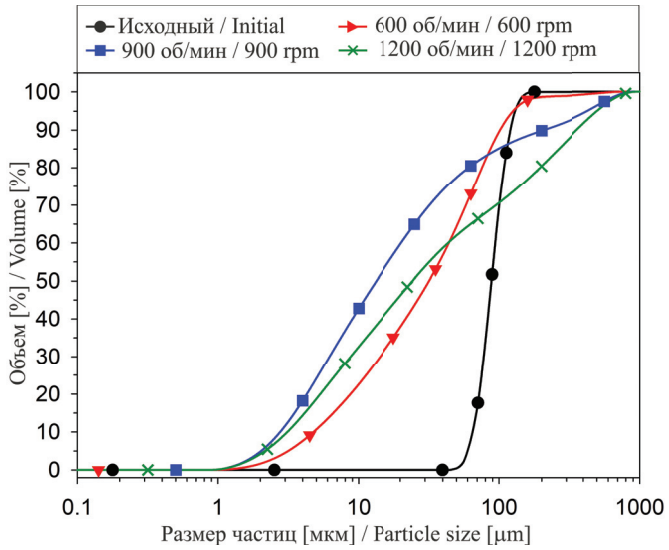

Fig. 4. Cumulative particle size distribution of the powder in the initial state and after high-energy milling using different rotational speed at a mass ratio of balls to the powder mass (BPR) of 100: 3

energy impacts led to higher plastic deformation. Furthermore, there was higher amount of cold-welded and deformed particles within the range of 200-700 μm as shown in Figure 3. Thus, it can be concluded, that the optimal rotational speed of initial molybdenum powder was found at 900 rpm.

The influence of distinct BPR and milling time on particle size

The next variable milling parameter under study was the ball to powder weight ratio with respect to the milling time. The rotational speed was 900 rpm and the time was set to: (i) 2 min of milling for samples 1A (BPR=100:3) and 6B (BPR=200:3); (ii) 5 min for 2A (BPR=100:3) and 7B (BPR=200:3); and (iii) 10 min for 8B (BPR=200:3). The changes in morphology for each powder are shown in Figure 5.

Sample 6B has smaller particle size (up to 56 vol.%) in comparison with the initial powder (see Figures 6 and 7). Cold-welded particles were also presented and had the size up to 550 μm, and amount up to 6.3

vol.%. Most of the particles had a size of 20 μm. On the other hand, sample 1A showed a greater number of cold-welded particles, i.e. the difference between particles fractured at the highest rotation frequency, with a size of about 300 μm, was about 10 vol.% for samples 1A and 6B. The volume fraction of finer particles was smaller in sample 1A in comparison with sample 6B up to 33 vol.%.

Samples milled for 5 min showed nearly the same morphology. The amount of finer and cold-welded particles was similar; the difference in the amount of finer particles between 2A (43 vol.%) and 7B (34 vol.%) was of about 9 vol.% (see Figures 6 and 7). The finer particles obtained at the highest mill speed had a size of about 20 μm at BPR=200:3 (7B) and about 30 μm at BPR=100:3 (2A). The main difference was in the amount of cold-welded particles. The lower amount (less than 6 vol.%) was achieved with higher BPR, while the higher amount (of about 18 vol.%) was revealed with the lower BPR.

For the longest milling time of 10 min and for BPR=200:3, the particle distribution changed. The initial powder particles were broken and the structure of milled powder was found finer (see Figure 5). The particle size with the highest frequency was 6 μm in the range size of 1-65 μm. The distribution of cold-welded particles remained almost the same in comparison with sample 7B (t=5 min and BPR=200:3). The cold-welded particles size with the highest frequency was of about 350 μm.

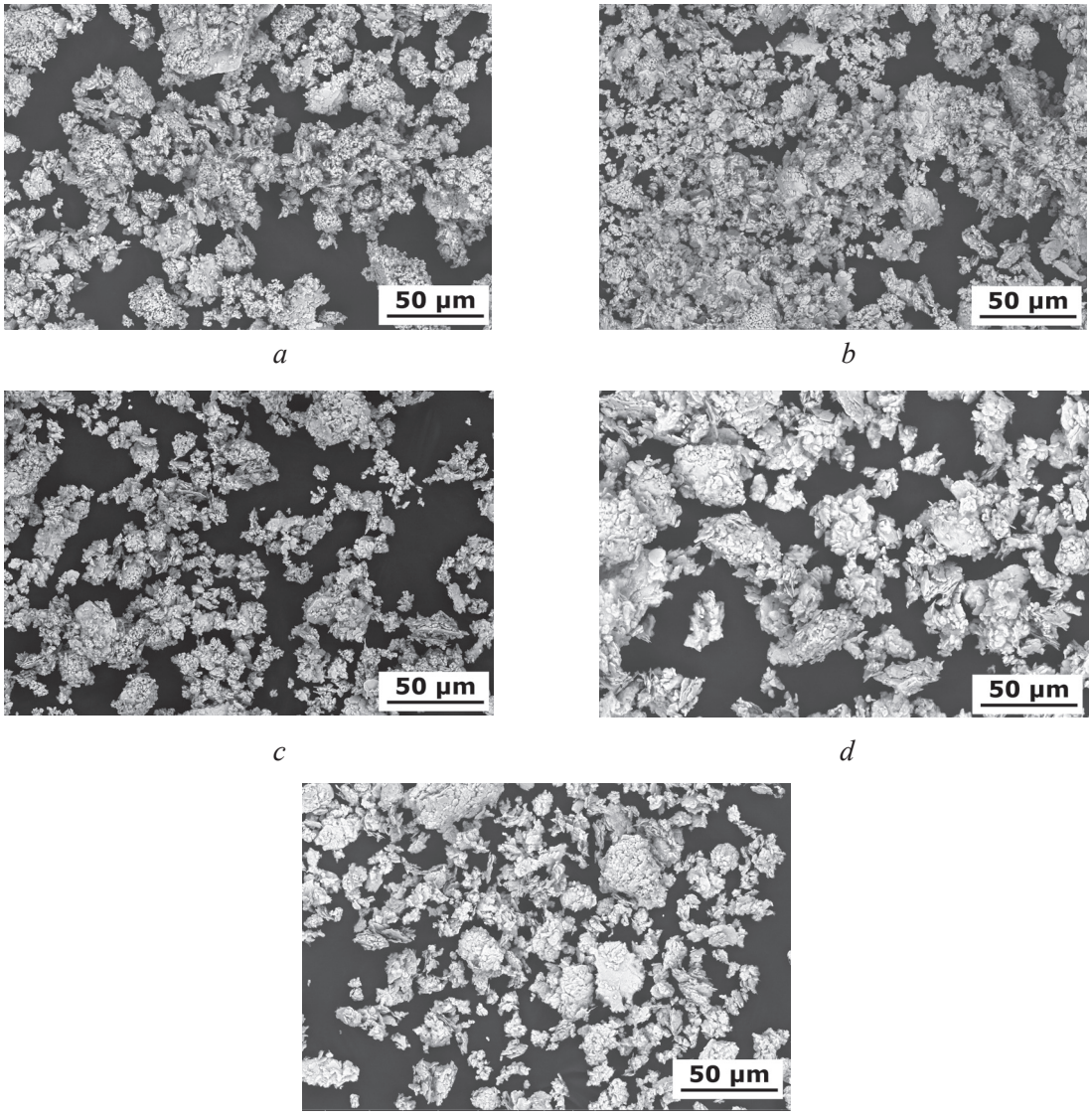

a *b* *c* *d* *e*

Fig. 5. High energy milled powder with variation in milling time and BPR, sample:
a – 1A (*t* = 2 min; BPR = 100:3); *b* – 2A (*t* = 5 min; BPR = 100:3); *c* – 6B (*t* = 2 min; BPR = 100:3); *d* – 7B (*t* = 5 min; BPR = 200:3); *e* – 8B (*t* = 10 min; BPR = 200:3), SEM-BSE

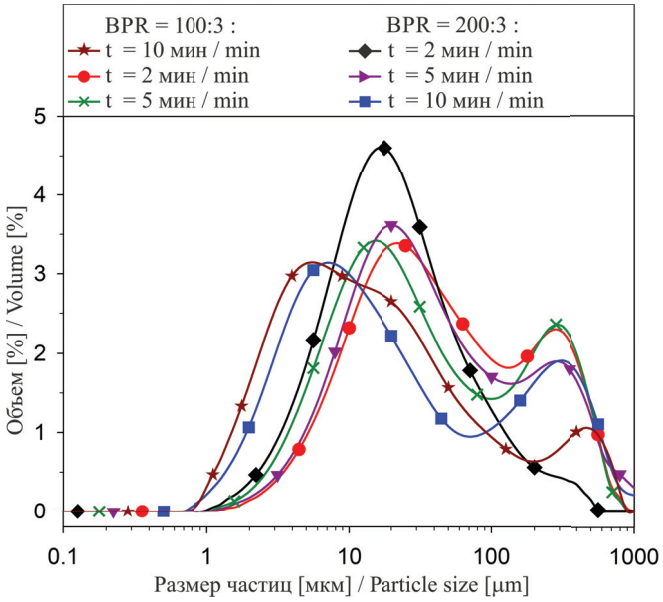

Fig. 6. The effect of BPR and milling time on the particle size of initial molybdenum powder at 900 rpm

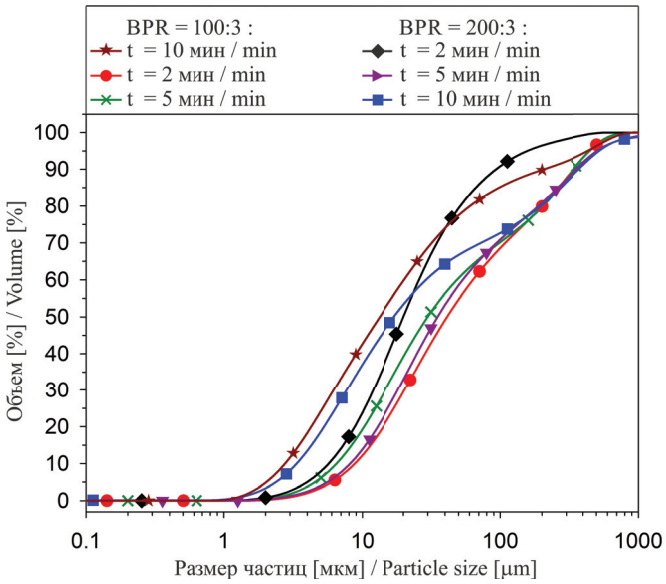

Fig. 7. The cumulative particle size distribution of the high energy milled powder at a different mass ratio of the balls to the powder mass (BPR) and the milling time at 900 rpm

The milled powder samples with higher milling time were 4A, 5A, 9B and 10B. The milling time was set to: (i) 30 min for sample 4A (BPR=100:3) and 9B (BPR=200:3), and (ii) 60 min for sample 5A (BPR=100:3) and 10B (BPR=200:3). All milled powders were analyzed by SEM and is shown in Figure 8.

Samples 4A, 5A and 10B showed a broad range of fine particles in the size range 1-100 μm (almost 80 vol.%), roughly in the same distribution (see Figure 9 and 10). These samples (4A, 5A and 10B) consisted from 50 vol.% of particles with size up to 20 μm, as depicted in Figure 8. The cold-welded particles were in each batch and were of about 200-1000 μm in size. Curve evolution for these samples was almost the same; however, sample 10B exhibited the finest particles in the submicron size range of 100-300 nm among all of milled powders.

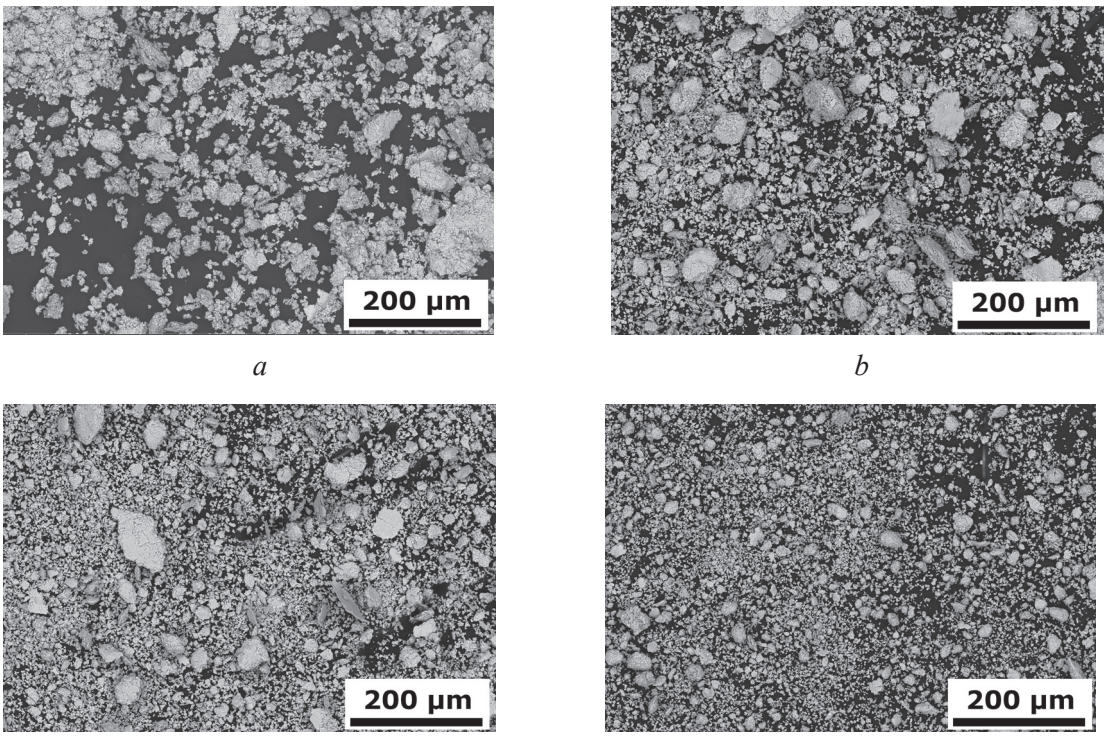

a *b*

c *d*

Fig. 8. High energy milled molybdenum powder with variation in BPR and milling time, samples:

a – 4A (*t* = 30 min; BPR = 100:3); *b* – 5A (*t* = 2 min; BPR = 100:3); *c* – 9B (*t* = 2 min; BPR = 100:3); *d* – 10B (*t* = 2 min; BPR = 100:3), SEM-BSE

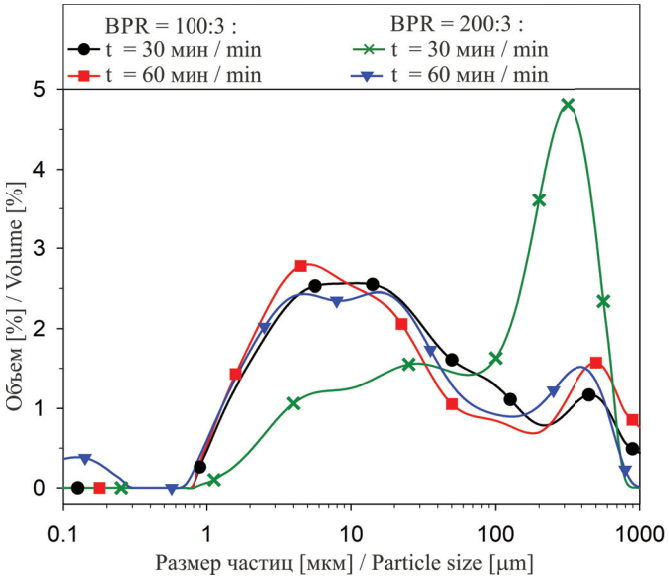

Fig. 9. The effect of BPR and milling time on the particle size of initial molybdenum powder at 900 rpm

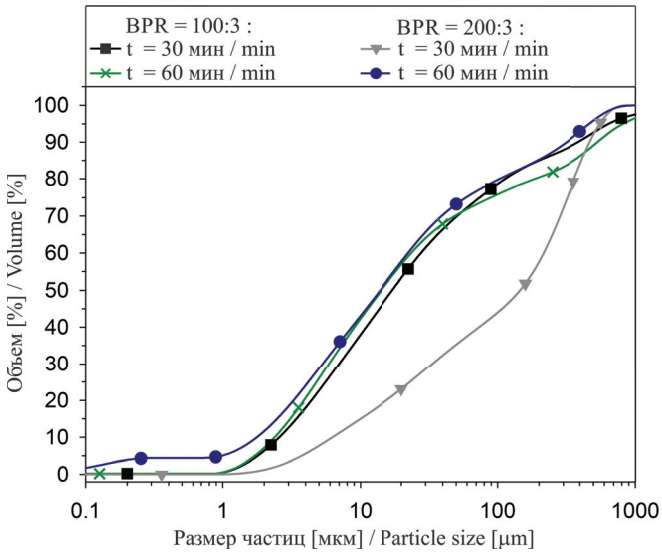

Fig. 10. Cumulative distribution of particle size of high energy milled powders utilizing different BPR and milling time at 900 rpm

The lowest amount (~40 vol.%) of these fine particles fraction in the size range of 1-100 μm and the highest amount (~50 vol.%) of cold-welded particles (size range 150-800 μm) were found in the sample produced using parameters 9B (see Figures 8, 9 and 10). Therefore, the cold-welded process and friction were predominant within these milling parameters.

Sample 10B (BPR 200:3 and 60 min) exhibited the most favorable morphology and granulometry. The finest powder particles with smaller cold-welded particles were achieved with the BPR (200:3) and the highest milling time (60 min) (see Figure 8d).

Herein, the optimization of a variety of milling parameters for molybdenum powder was studied. The influence of rotational speed, BPR and milling time on the particle size, was investigated and evaluated.

The milling speed was set up to (i) 600 rpm, (ii) 900 rpm and (iii) 1200 rpm. The lowest speed (600 rpm) exhibited partially broken particles through the repeated deformations and fractures with the small amount of fine particles. However, the certain amount (32 vol.%) of agglomerated particles remained the same in size as at the beginning (100 μm). The milling efficiency was not sufficient in this case. The next rotational speed was 900 rpm. Initial powder particles were totally fractured so the particles were finer and in the size range of 12-200 μm. Cold-welded particles (~13 wt.% in the size range 200-600 μm) were also presented. At higher milling speed, the highest amount (up to 60 vol.%) of finer particles was achieved. Under the highest milling speed of 1200 rpm, the plastic deformation was increased and the cold-welding process was minimized. As a result, flake-like powder particles appeared in 35 vol.%. The size of these particles was within the range of 200 to 700 μm. With this milling speed, the kinetic energy led to the higher plastic deformation which caused coarse flake-like particles. A similar situation was reported by Biyik and Aydin, who achieved flake-like morphology on copper and tungsten powder at the highest speed because of the higher plastic deformation and the lower fracturing of particles, [24]. Based on the results obtained, it can be concluded that the optimal rotation speed is 900 rpm.

The next set of experiments was carried out at 900 rpm, and the milling time and BPR were varied. Samples with a constant BPR and a longer processing time showed that the amount of cold-welded particles decreased, while its sizes increased. The particle size has decreased, and its number has increased, while the range of sizes of these particles has become wider, which shows a wide peak (Fig. 9). The decreased amount of cold-welded particles and higher amount of finer particles were caused due to the fact that powder particles were more preferably fractured than cold-welded. Similar behavior was also found for Suryaanarayana and Razavi-Tousi et al., where the particle size of powder increased at the beginning of milling process due to the cold welding process [20, 25]. Consequently with longer milling time, the particle

size decreased because of predominance of fracture mechanism [20, 25]. One exception was achieved during milling with BPR=200:3 for 30 min, where the cold-welding process was predominant. In this case, the cold-welded particles were included in 50 vol.%, while fine particles approximately in 40 vol.%. According to [25], it can be stated, that this milling time was closed to steady state and longer milling time would have a negligible effect on the change of the overall trend of evolution of particles. Ravazi-Tousi et al. also suggested that the change in the milling condition influences the milling time when a system reaches steady state. In our case for set milling parameters, the change of BPR influenced the time when the system almost reached the steady state.

Samples with constant time and different BPR (200:3 and 100:3) showed that the higher the BPR (200:3) was, then the powder particles were finer and the efficiency of milling process was increased. So it can be assumed that the higher efficiency of milling process was caused by a higher amount of collisions and within particles increased friction. Kilinc et al. also obtained similar results in their experimental work, where they investigated milling characteristics of alumina powders for different (i) BPR of 5:1, 10:1, 20:1 and 40:1, (ii) milling time (1, 5, 10 and 15 h) and (iii) rotational speed (500, 700 and 900 rpm), [26]. They found that with increasing milling time and BPR, the powder particles were finer. On the other hand, it should be mentioned, that the efficient BPR isn't always the highest one, because the higher number of balls can affect the movements of the balls in negative way.

Conclusions

The optimization of a variety of milling parameters, such as the rotational speed, the milling time and BPR, were investigated and determined and the following conclusions can be stated:

- The most optimal rotational speed was 900 rpm which exhibited the highest amount (~60 vol.%) of fine particles up to the size of 20 μm. However, a certain amount of cold-welded particles were also presented.
- Using a higher BPR (200:3) resulted in smaller particles compared to samples with a low BPR (100:3). Thus, it can be assumed that the greatest efficiency of the milling process was achieved by using a larger value of the BPR parameter (200:3), where the number of high-energy collisions of powder particles and milling bodies was greater.
- Increasing the milling time led to a reduction in the particle size of the powder and to a decrease in the number of cold-welded particles. The maximum reduction in the particles size was achieved by milling for 10 min with BPR=200:3. The particle size was reduced from initial size of 100 μm to the submicron size range of 100-300 nm.
- The best uniformity of milled powders was achieved at BPR=200:3 and a milling time during 60 min.

References

1. Neikov O., Naboychenko S., Murashov I.B., Yefimov A., Dowson G. *Handbook of Non-ferrous metal powders: technologies and applications*. Amsterdam, Elsevier Science, 2009, pp. 464–470.

2. Dean J.A. *Lange's handbook of chemistry*. New York, McGraw-Hill Professional, 1998.

3. Davis J.R., ed. *ASM speciality handbook. Heat resistant materials*. Materials Park, Ohio, ASM International, 1997, pp. 361–364.

4. Ohser-Wiedemann R., Martin U., Seifert H.J., Müller A. Densification behavior of pure molybdenum powder by spark plasma sintering. *International Journal of Refractory Metals and Hard Materials*, 2010, vol. 28. iss. 4. pp. 550–557. doi: 10.1016/j.ijrmhm.2010.03.003.

5. Kim Y., Lee S., Noh J.-W., Lee S.H., Jeong I.-D., Park S.-J. Rheological and sintering behaviors of nanostructured molybdenum powder. *International Journal of Refractory Metals and Hard Materials*, 2013, vol. 41, pp. 442–448. doi: 10.1016/j.ijrmhm.2013.06.001.

6. Sheng Y., Guo Z., Hao J. Characterization of spherical molybdenum powders prepared by RF plasma processing. *Advanced Materials Research*, 2012, vol. 482–484, pp. 2563–2567. doi: 10.4028/www.scientific.net/AMR.482-484.2563.

7. Liu X.-P., Wang K.-S., Hu P., Chen Q., Volinsky A. Spheroidization of molybdenum powder by radio frequency thermal plasma. *International Journal of Minerals, Metallurgy and Materials*, 2015, vol. 22, iss. 11, pp. 1212–1218. doi: 10.1007/s12613-015-1187-7.

8. Garg P., Park S.-J., German R.M. Effect of die compaction pressure on densification behavior of molybdenum powders. *International Journal of Refractory Metals and Hard Materials*, 2007, vol. 25, iss. 1, pp. 16–24. doi: 10.1016/j.jrmhm.2005.10.014.

9. Leitner K., Felfer P.J., Holec D., Cairney J., Knabl W., Lorich A., Clemens H., Primig S. On grain boundary segregation in molybdenum materials. *Materials & Design*, 2017, vol. 135, pp. 204–212. doi: 10.1016/j.matdes.2017.09.019.

10. An G., Sun J., Liu R.-Z., Li J., Sun Y.-J. Mechanical properties of molybdenum products prepared by using molybdenum powders with different micro-morphologies. *Rare Metals*, 2015, vol. 34, iss. 4, pp. 276–281. doi: 10.1007/s12598-013-0194-y.

11. Yang Ch., Zhou Y., Liu D., Jiang W., Liu F., Liu Z. Preparation of molybdenum powder from molybdenite concentrate through vacuum decomposition-acid leaching combination process. *Rare Metal Technology*. Cham, Springer, 2017, pp. 235–246.

12. Bolitschek J., Luidold S., O'Sullivan M. A study of the impact of reduction conditions on molybdenum morphology. *International Journal of Refractory Metals and Hard Materials*, 2018, vol. 71, pp. 325–329. doi: 10.1016/j.ijrmhm.2017.11.037.

13. Kim Y., Lee S., Noh J.-W., Lee S.H., Jeong I.-D., Park S.-J. Rheological and sintering behaviors of nanostructured molybdenum powder. *International Journal of Refractory Metals and Hard Materials*, 2013, vol. 41, pp. 442–448. doi: 10.1016/j.ijrmhm.2013.06.001.

14. Wang D., Yu Ch., Ma J., Liu W., Shen Z. Densification and crack suppression in selective laser melting of pure molybdenum. *Materials and Design*, 2017, vol. 129. pp. 44–52. doi: 10.1016/j.matdes.2017.04.094.

15. Ghayour H., Abdellhi M., Bahmanpour M. Optimization of the high energy ball-milling: modeling and parametric study. *Powder Technology*, 2016, vol. 291, pp. 7–13. doi: 10.1016/j.powtec.2015.12.004.

16. Liu M., Zhong X., Wang J., Liu Z., Qui W., Zeng D. Microstructure and thermal stability of MoSi2-CoNiCrAlY nanocomposite feedstock prepared by high energy ball milling. *Surface and Coatings Technology*, 2014, vol. 239, pp. 78–83. doi: 10.1016/j.surfcoat.2013.11.022.

17. Harris J.R., Wattis J.A.D., Wood J.V. A comparison of different models for mechanical alloying. *Acta Materialia*, 2001, vol. 49, iss. 19, pp. 3991–4003. doi: 10.1016/S1359-6454(01)00302-0.

18. Karthik B., Gautam G.S., Karthikeyan N.R., Murty B.S. Analysis of mechanical milling in simoloyer: an energy modeling approach. *Metallurgical and Materials Transactions A*, 2012, vol. 43, iss. 4, pp. 1323–1327. doi: 10.1007/s11661-011-0946-y.

19. Debata M., Acharya T.S., Sengupta P., Acharya P.P., Bajpai S., Jayasankar K. Effect of high energy ball milling on structure and properties of 95W-3.5Ni-1.5Fe heavy alloys. *International Journal of Refractory Metals and Hard Materials*, 2017, vol. 69, pp. 170–179. doi: 10.1016/j.ijrmhm.2017.08.007.

20. Suryaanarayana C. Mechanical alloying and milling. *Progress in Materials Science*, 2001, vol. 46, iss. 1–2, pp. 1–184. doi: 10.1016/S0079-6425(99)00010-9.

21. Ebrahimi-Kahrizsangi R., Abdellahi M., Bahmanpour M. Ignition time of nanopowders during milling: a novel simulation. *Powder Technology*, 2015, vol. 272, pp. 224–234. doi: 10.1016/j.powtec.2014.12.009.

22. Kiran U.R., Kumar M.P., Sankaranarayana M., Singh A.K., Nandy T.K. High energy milling on tungsten powders. *International Journal of Refractory Metals and Hard Materials*, 2015, vol. 48, pp. 74–81. doi: 10.1016/j.ijrmhm.2014.06.025.

23. Abdellahi M., Bhmanpour M., Bahmanpour M. Optimization of process parameters to maximize hardness of metal/ceramic nanocomposites produced by high energy ball milling. *Ceramics International*, 2014, vol. 40, iss. 10, pp. 16259–16272. doi: 10.1016/j.ceramint.2014.07.063.

24. Biyik S., Aydin M. The effect of milling speed on particle size and morphology of Cu25W composite powder. *Acta Physica Polonica A*, 2014, vol. 127, pp. 1255–1260.

25. Rzavi-Tousi S.S., Szpunar J.A. Effect of ball size on steady state of aluminum powder and efficiency of impacts during milling. *Powder Technology*, 2015, vol. 284, pp. 149–158. doi: 10.1016/j.powtec.2015.06.035.

26. Kilinc Y., Öztürk S., Öztürk B., Uslan I. Investigation of milling characteristics of alumina powders milled with a newly designed vibratory horizontal attritor. *Powder Technology*, 2004, vol. 146, pp. 200–205. doi: 10.1016/j.powtec.2004.09.031.

Conflicts of Interest

The authors declare no conflict of interest.